8.3 Transferability of Insights from Fundamental Investigations into Practical Applications of Prechamber Combustion Systems

Panagiotis Kyrtatos, Konstantinos Bardis, Michele Bolla, Alexey Denisov, Yuri Wright, Kai Herrmann, Konstantinos Boulouchos

Abstract

Efforts to reduce CO_2 emissions from spark ignition engines have driven engine development to lean-burn or high-dilution operation, which results in high combustion variability as well as increased unburned hydrocarbon emissions. A widely used technology to reduce these issues are prechamber ignition systems, in which the external ignition source is located in a separate small volume, connected to the main chamber via small orifices. This setup allows for design of favourable ignition conditions near the ignition source, which results in fast and repeatable early flame propagation. The pressure increase resulting from combustion taking place inside the prechamber leads to the ejection of jets containing hot combustion products and possibly active radicals into the main chamber, which ignite the lean or diluted mixture; this process is often dubbed turbulent jet ignition or TJI. The use of TJI systems in engines allows the combustion of very lean/diluted mixtures, resulting in higher efficiencies and lower NOx emissions.

In this work we shed light into the importance of quenching for practical applications involving turbulent jet ignition. This is achieved through optical investigations in a generic, constant volume test-rig, combined with zero-dimensional (0-D) model calculations. The 0-D model is applied to the generic setup and in real engine applications under varying operating conditions, in order to highlight the relative importance of quenching under the various thermochemical conditions encountered. The results indicate that thermal quenching in the nozzle should not be expected due to the small flame thickness under high pressure encountered in internal combustion engines. Nevertheless, under the jet mixing conditions expected in engines, hydrodynamic quenching due to mixing of burned products with unburned (cold) main chamber mixture can be expected. In most engine conditions, the re-ignition process of the initially quenched jet after their exit from the prechamber is expected to be so fast, that quenching will not be apparent in most measurements.

1 Introduction

Efforts to reduce CO_2 emissions from internal combustion engines have led to the use of natural gas as a fuel in lean-burn spark ignition engines. Lean-burn, or alternatively high-dilution combustion concepts, are employed to keep engine efficiency high by minimizing thermal losses, while simultaneously ensuring NOx emissions below legislated limits. Under high-dilution conditions, operation is limited by high cyclic variability as well as increased unburned hydrocarbon emissions [1, 2]. In order to address these

limitations, external ignition engines require high ignition energy and distributed ignition sources in order to ignite and consume the lean/diluted premixed main charge [1, 3].

A technology widely used in these engines is the prechamber ignition system, in which the external ignition source is located in a separate small volume, connected to the main chamber via small orifices [1, 2]. This setup allows for design of favorable conditions near the ignition source, in particular controlled flow properties (absence of large scale bulk motion) and turbulence levels, which result in fast and repeatable early flame propagation. The pressure difference resulting from combustion taking place inside the prechamber pushes jets containing active radicals and/or hot combustion products into the main chamber, which ignite the lean or diluted mixture; this process is often dubbed turbulent jet ignition or TJI. The use of TJI systems in engines allows the combustion of very lean/diluted mixtures, resulting in higher efficiencies and lower NOx emissions. Research in the field of prechamber combustion has been extensive in the past years, aiming to increase our understanding of turbulent jet ignition systems. These studies have ranged from fundamental investigations of turbulent jet ignition under atmospheric conditions [4-7], to optical experiments [8-12] and simulations [8, 12-16] in engine or engine-like setups.

Biswas et al. [4] studied TJI in a generic single-hole prechamber configuration employing simultaneous high-speed Schlieren and OH*-chemiluminescence imaging. The authors identified two distinct main chamber ignition patterns depending on the ignition time and the flame morphology, which they coined “flame ignition” and “jet ignition”. In addition, they introduced a “global” Damköhler number based on the relationship between laminar flame speed and turbulence at the nozzle, which they used to explain cases where no main chamber ignition was observed. Yamaguchi et al. [5] also studied ignition in a divided chamber bomb. Based on the physical and chemical characteristics of the torch jet, ignition was classified into four different types. Other researchers [6, 7, 14, 17] carried out fundamental studies of mixture ignition via a hot jet, concluding that scalar dissipation rate and flame thickness are of vital importance for the process of ignition and the resulting ignition delay. Recent studies from Mastorakos et al. [18] and Allison et al. [19] were carried out in a constant volume chamber connected to the environment via a small orifice, resembling a prechamber-main chamber setup. They reported a curvature-induced quenching at the nozzle due to the high speed jet and the limited effective nozzle diameter.

All abovementioned investigations [4-7, 14, 17-19], have been performed under thermodynamic conditions (in particular pressure) which are significantly different to conditions encountered in typical internal combustion engine. Despite the fact that relevant observations concerning the phenomenology of TJI can be made in such investigations, there is no established framework to compare the conditions as well as the phenomenology with engine conditions; i.e. the practical relevance of the observed phenomenology and conclusions can be demanding to determine.

Recent work from the current authors has focused on optical investigations in a rapid compression-expansion machine [8, 20, 21], where engine relevant conditions can be attained Optical results using simultaneous high-speed Schlieren imaging and OH* chemiluminescense showed that the appearance of a reactive flame (non-negligible signal in the OH* chemiluminescense images) was observable near the prechamber nozzle exit, and was concurrent with the exiting of hot jets from the prechamber. This

indicates that under engine-relevant conditions, prechamber flame does not completely quench as it passes through the nozzles, and thus the use of a level-set combustion model TJI and the combustion process is justified.

In traditional spark ignition engines, flame quenching is rarely very important, since conditions typically encountered do not lead to quenching. For this reason, flame quenching is often completely neglected in spark ignition simulations, or accounted for in a very simplified way. Nevertheless, flame quenching mechanisms constitute a topic of fundamental interest, with relevance in many practical applications.

In the present study, we aim to shed light into the importance of quenching for practical applications involving turbulent jet ignition. This is achieved through optical investigations in a generic, constant volume test-rig, combined with 0-D model calculations (previously presented in [22]) in the generic setup and in real engine applications under varying operating conditions. Through this investigation we aim to highlight the relative importance of quenching under different conditions in fundamental test rigs and practical applications. This information will aid to evaluate the errors induced by neglecting quenching in TJI setups depending on the operating conditions. In the future, this information can possibly lead to improvements in the level-set methods (such methods, the most common of which is the G-equation model, have inherent limitations in simulating flame total or partial quenching) currently used for most simulations in an industrial context, as well as encourage the use of more physically accurate flame models in TJI simulation applications.

2 Flame quenching and re-ignition mechanisms

Quenching in a turbulent reacting jet passing through a nozzle into a chamber with unburned (cold) mixture can occur due to two distinct mechanisms. One is thermal quenching, whereby the heat losses towards the nozzle wall exceed the heat release of the flame. The second mechanism, named hydrodynamic quenching, is caused by the intense mixing of the products of combustion emanating from the prechamber with the cold unburned mixture found in the main chamber. Both mechanisms are depicted schematically in Figure 1.

Thermal quenching caused by wall heat losses may be relevant in TJI applications due to the large surface-to-volume ratio within the nozzle and the strong interaction with the nozzle walls during the passage of the flame front through it. The phenomenon of wall quenching refers to the inability of a flame to sustain wall heat losses below a certain distance from the wall. The critical distance below which flame quenches (δ_q) over the flame thickness (l_f), is referred to as the Peclet number (Pe).

$$Pe = \frac{\delta_q}{l_f} \approx 10 \quad \text{(side wall quenching, according to [23])} \tag{1}$$

The equation above indicates that quenching will be more probable when the flame thickness is high (low chamber pressure) or the nozzle is very narrow.

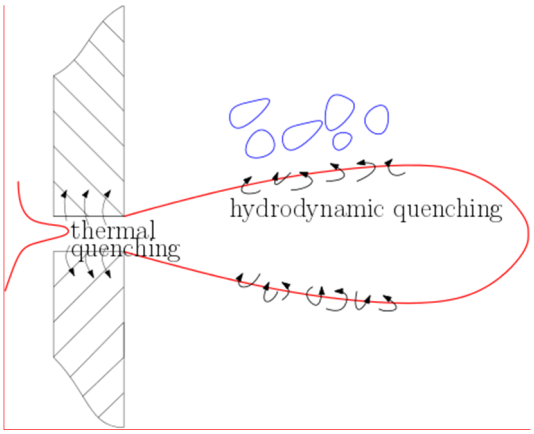

Figure 1: Schematic of the different quenching mechanisms encountered in turbulent jet ignition applications

Hydrodynamic quenching is the process whereby the flame quenches due to reduced temperature from strong mixing with the cold unburned gases. To determine the propensity of quenching by mixing we evaluate:

$$Da = \frac{\tau_{mix}}{\tau_{fl}} = \frac{\frac{l_I}{u'}}{\frac{l_f}{S_l}} \tag{2}$$

which is the non-dimensional Damköhler number (Da) of the relative chemical reactions intensity compared to mixing. Due to the time and space-varying nature of turbulence within a jet, the evaluation of a single Damköhler number is not straightforward for such a case. For the present investigation we choose to evaluate Da sufficiently downstream the nozzle exit (five nozzle diameters), where turbulence has already developed [24].

In detail, the integral length scale (l_I) is evaluated based on the nozzle diameter for a steady state jet, while the turbulent intensity (u') is based on the nozzle velocity. The two estimates provided here are derived from [24] and [25] respectively:

$$l_I = 0.2\, d_{noz} \tag{3}$$

And

$$u' = 0.1\, u_{noz} \tag{4}$$

Hydrodynamic quenching takes place, irrespective of the specific thermochemical conditions and fuel properties, if the aforementioned number drops below a critical threshold $Da_{cr} \approx 0.5$. This assumption for the critical Da is based on previously published results in similar configurations [4] and [26]. Although this evaluation of Da and Da_{cr} does not provide a solid indication of quenching, it can serve as a basis for comparison of different setups and operating conditions.

While the abovementioned criteria for flame quenching give an indication of the quenching probability, they do not offer insights into whether or not the mixture will ignite – and if so, how fast – once quenched. This information would be important to

judge whether quenching, if it occurs, can actually have a profound effect on the combustion, or whether it can be neglected. In cases where reactivity is very high and re-ignition is imminent, the assumption of no quenching might adequately depict reality, and can possibly be used in 3D CFD and 0-D simulations without introducing significant error. In this perspective, a simplified ignition delay time for a homogeneous mixture consisting of unburned and burned gases can be computed, which can serve as a proxy for eventual ignition processes:

$$\tau_{ign} = f(p, Tu, Tb) \tag{5}$$

This quantity can be calculated using perfectly stirred reactors (PSR) with a presumed mixture of burned and unburned gases. Having calculated the reactant temperature for the products of combustion, the PSR initial temperature is given as a function of unburned mixture fraction (ξ) assuming adiabatic mixing of the burned and unburned gases. This allows the calculation of the ignition delay for different ξ, which will tend to zero at ξ=1 (fully burned products). This simplified approach neglects the effect of combustion radicals coming from the prechamber on main chamber ignition; these effects can only be taken into account using significantly more complex physicochemical modelling, which is beyond the scope of this work.

A small ignition delay indicates that re-ignition is likely to occur under the given thermochemical conditions. In contrast, a mixture with high ignition delay will most likely not reignite before the temperature of the burned gases drops significantly by the action of heat losses and mixing.

3 Zero Dimensional Simulations

To address the questions presented above and to further enhance the understanding of the experimentally observed combustion modes, simulations have been performed using a zero dimensional model. Another objective for the use of the 0-D model is to enable the comparison of the fundamental experiments with engine conditions, through the comparison of the TJI characteristics in a typical engine. This will allow the determination of the transferability of findings obtained from fundamental investigations to practical applications.

Although the complete formulation of the 0-D model is beyond the scope of the present publication, some basic information regarding the model will be given for completeness. The 0-D model assumes that the PC mixture is separated into two zones; a burned zone behind the flame front position and an unburned zone ahead of the flame front. A simplified description of the pre chamber geometry as well as of the flame front is adopted to reduce complexity, while, still, preserving the main features of the pre chamber.

A coupled system of differential equations is solved to obtain the thermodynamic variables, such as pre and main chamber pressure and temperature. The heat release rate is modelled based on the active flame front area and a turbulent flame speed. Turbulence intensity inside the pre chamber, which is relevant only for the engine ap-

plication, is modelled using a refined 0-D turbulence sub-model obtained via a reduction of the well established CFD k-ε model. The latter model has been extensively validated with 3D-CFD simulations in a previous publication [22].

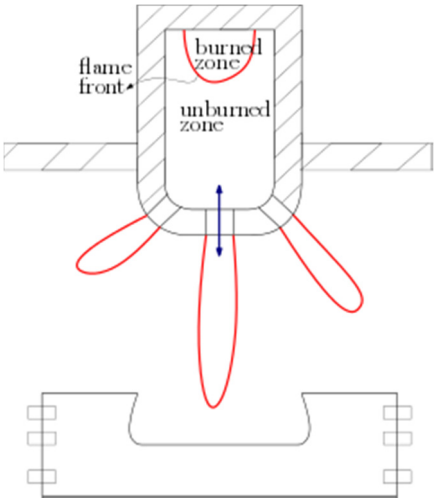

Figure 2: Schematic of the 0-D model zones in the pre and main chambers

The present publication focuses on the determination of the conditions near the nozzle exit and during the early phase of main chamber combustion, when the main chamber heat release rate does not significantly change the conditions in the main chamber; therefore, only the pressure difference between the pre and main chamber is of interest. In addition, the physical parameters that involve the computation of the flame speed and flame thickness are evaluated with respect to the unburned zone and, consequently, the main chamber burned zone properties are not of interest.

4 Experimental Setup and Operating Conditions

A newly developed, constant volume divided combustion chamber, named the optically accessible prechamber (OPC), has been designed and built to allow the study of TJI under different operating conditions. The test-rig contains two volumes, which are connected through a single interchangeable orifice. The smaller of the two volumes, (identified as the prechamber), contains an ignition source (sparkplug), which allows the ignition of the mixture. The orifice connecting the prechamber to the main chamber can be changed in shape and diameter, and can fit a nozzle with a maximum diameter of 4 mm. In the configuration used in this investigation, the volume of the main chamber is 186’988 mm^3, whereas the prechamber is 3’602mm^3 (~1.9% of the total volume).

Both chambers have windows to allow optical access into the respective volumes, which enable optical measurements during the combustion event. The prechamber is fitted with two opposing windows, which allow optical access through the complete prechamber volume. The main chamber also has two opposing windows, allowing optical access from the nozzle exit to the bottom of the chamber. A removable opposing wall is placed 40 mm away from the nozzle exit.

The operation and control sequences of the OPC allow the accurate setting of conditions in both chambers prior to ignition, cf. Table 1 unterhalb. The charge air pressure and temperature is feedback controlled through an intake and leakage valve system,

and an electrical heating system. The fuel in the main chamber is injected using a hollow-cone piezo injector, and the mixture composition is determined using the pressure signal and a partial pressure calculation. An external mixing tank is used to prepare the mixture for the prechamber, allowing the separate setting of composition in the two chambers. The premixed mixture is injected directly into the prechamber prior to ignition. The fuel used in this study is pure methane (N45, ≥ 99,995 mol %).

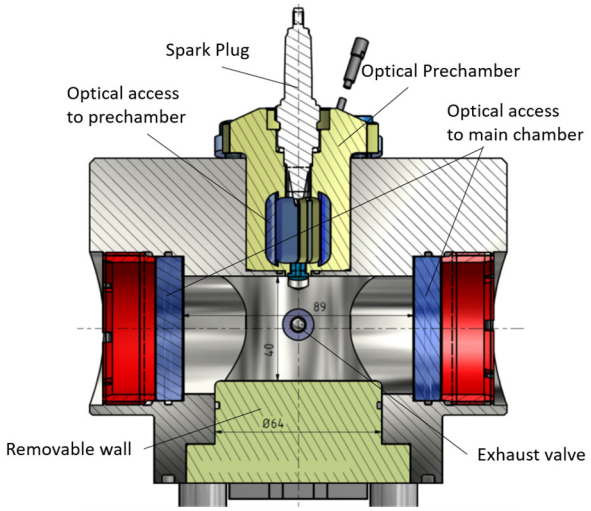

Figure 3: Schematic of the Optical Prechamber, showing the main parts

The operating conditions possible for the current setup are presented in Table 1.

Table 1. Operating conditions possible in the OPC

Parameter	Unit	Value
Initial Pressure	bar	1…20
Initial Temperature	K	300…450
Φ Prechamber		0…>5
Φ Main Chamber		0…>5

Information about the combustion characteristics of the turbulent jet emanating into the main chamber was recorded using a simultaneous high-speed Schlieren and 2D OH* chemiluminescence imaging setup. For this purpose, two LaVision HSSX high-speed cameras were used, set at a frame rate of 20 kHz. For OH* an image intensifier was fitted to the camera, in addition to a bandpass filter for a wavelength of 306 nm.

For the comparison of the OPC fundamental TJI investigations with practical engine conditions, results from a near-production Liebherr full metal test engine were used. The engine is a lean burn, medium-speed engine, equipped with chamber sparkplugs with five nozzles, of which four are peripheral and one axial. The axial nozzle is mainly applied for efficient scavenging and convection of the swirl vortex towards the spark plug. Additional information concerning the engine and experimental conditions used can be found in [15, 22].

5 Results

The present section contains the experimental results from the optical prechamber, followed by the simulations of the OPC and engine conditions. The experimental results include a brief description of the 0-D model validation. The 0-D model is used in both experimental setups in order to obtain the relative time scales and non-dimensional numbers, which allow the comparison of the two setups.

5.1 Optical Prechamber

The optically accessible prechamber constant volume setup is used in order to evaluate the propensity of jet flame quenching and re-ignition. Three distinct operating conditions were chosen in order to highlight the effect of jet mixing and thermodynamic conditions on flame quenching and the subsequent re-ignition.

The operating conditions chosen for the investigation are summarized in Table 2. The conditions differ in terms of nozzle diameter (d_{noz}=4 mm for case 1, 2 mm for cases 2 and 3) and initial charge temperature (T_{in}=~300 K for cases 1 and 2, ~430 K for case 3), with constant initial pressure (P_{in}=~5 bar), as well as prechamber and main chamber compositions (Φ_{PC}=~1 and Φ_{MC}=~0.75, respectively). The values stated are the average of the individual repetitions recorded for each operating condition (5 for case 1, 7 for cases 2 and 3). Temperature is expected to affect significantly the mixture reactivity and consequently the flame speed and ignition propensity. Higher mixture reactivity results in increased nozzle velocity and, therefore, temperature influences both terms of the Damköhler number. The different nozzle diameters significantly modify the mixing Damköhler number through changes in jet velocity.

Table 2. Operating conditions used for the investigation in the OPC

Case No.	P_{in} (bar)	T_{in} (K)	d_{noz} (mm)	Φ_{MC}	Φ_{PC}	No. of Repetitions
1	5.67	302	4	0.75	0.97	5
2	5.13	299	2	0.75	0.92	7
3	5.16	434	2	0.74	0.94	7

The experimental results are presented in the figures below. Figure 4 shows the measured main chamber pressure (blue, left axis), along with the pressure difference between main chamber and prechamber (red, right axis), plotted against time after ignition for the three OPC cases. All repetitions are plotted for each case, showing good repeatability of the conditions.

Figure 5 shows the Schlieren images (in green/black) from the main chamber, with the OH* chemiluminescence overlaid, for significant time-instances for the same three cases. The images are taken from a representative repetition of the experiment, chosen as the cycle with pressure closest to the average of all cycles at the same conditions. Note that the different images do not correspond to the same time instances for the different cases, since the timings of the hot jet exit and subsequent ignition differ significantly between different conditions. Also note that the OH* is only shown as a binary value above a certain arbitrary threshold, which is chosen to remove signal

noise. This binary value allows comparison of the locations of significant OH* luminosity, permitting the determination of reaction zones and enabling identification of flame quenching and re-ignition.

In case 1, minimal pressure increase is observed in the prechamber, while the main chamber ignition happens very quickly after the hot jet exit. The burned products are first observed in the main chamber at 5.5 ms after ignition (see Figure 5), with some OH* visible immediately. The hot jet then propagates through the main chamber and hits the opposing wall, with the tip of the jet showing no OH* signal, indicating flame quenching due to mixing. The main chamber pressure shows significant increase only after 7.2ms, which is also where a broader OH* signal is observed.

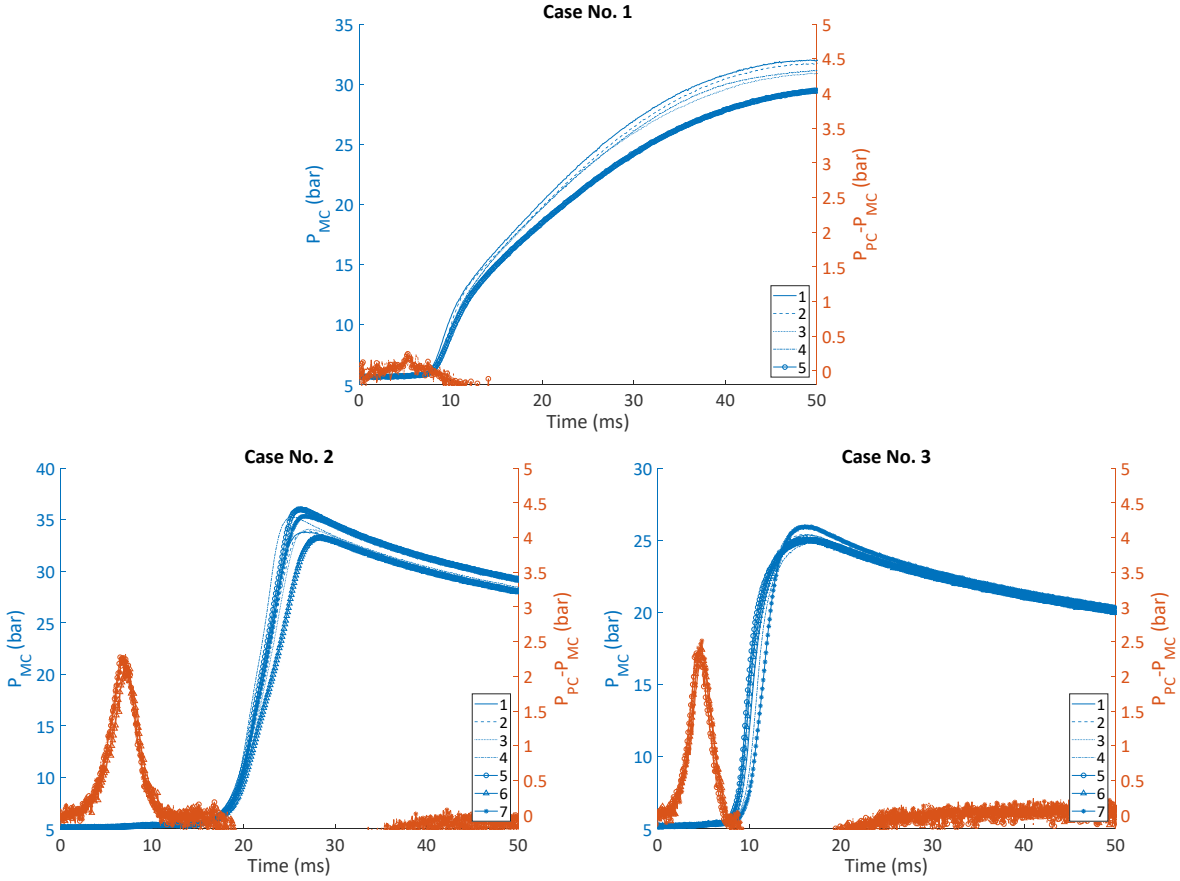

Figure 4: Measured main chamber pressure (blue, left axis) and prechamber minus main chamber pressure difference (red, right axis) plotted over time after ignition for all repetitions of the OPC cases 1-3

In cases 2 and 3 the pressure increase in the prechamber is much sharper, due to the lower cross-sectional area of the nozzle (D_{noz}=2 mm). In case 2 the PC pressure peak is delayed due to the less reactive mixture conditions compared to case 3 ($T_{in,2}$=300 K vs $T_{in,3}$=430 K). The main chamber ignition is also delayed for the same reasons. In both cases, the initial hot jet exit does not show any OH*, indicating complete flame quenching within the nozzle or in the main chamber.

In case 2 the hot jet is first observed in the main chamber 5.95 ms after ignition, with the jet penetrating fast in the main chamber and hitting the opposing wall. Early penetration Schlieren images (e.g. at 6.3 ms) show very low Schlieren signal near the jet

tip, indicating very low temperature gradients and thus very strong mixing at that location. The fist OH* signal is observed at the jet core near the nozzle after 9.65 ms, which is when the pressure difference between the two chambers and thus the jet velocity falls to very low values. The OH* signal then completely disappears before significant signal is observed again at around 13 ms at different locations along the jet. Significant main chamber pressure increase indicating heat release and widespread OH* signal are only observed after 15 ms, resulting in a total ignition delay between hot jet exit and widespread ignition of ~9 ms.

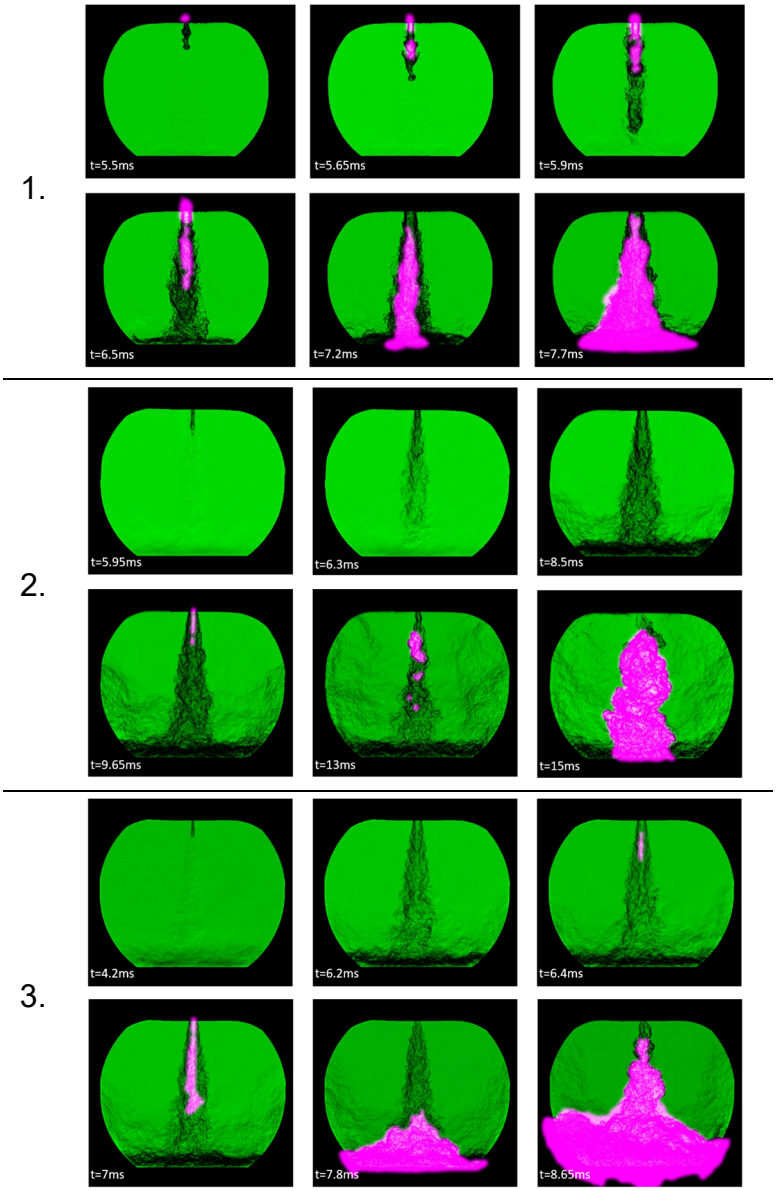

Figure 5: Optical images of the main chamber, showing the Schlieren image (green/black) with superimposed OH (pink) for one repetition of the OPC cases 1 (upper), 2 (middle) and 3 (lower series)*

The jet in case 3 shows a similar behavior to case 2, but with an accelerated sequence of events. The hot jet exit is observed at 4.2 ms, followed by the first OH* signal at 6.4 ms near the nozzle exit. The OH* area then expands and is finally convected towards the wall, before widespread ignition and main chamber pressure increase after 8.3 ms. The ID in this case is shorter than case 2, and is ~4 ms.

Overall, what we observe is that in case 1, there still exists a reaction zone at the nozzle exit, as indicated by the OH* signal, suggesting no complete quenching within the nozzle. The flame is nevertheless quenched downstream of the nozzle, when the hot products mix sufficiently with the cold unburned gases in the main chamber, suggesting quenching due to mixing. In cases 2 and 3 we observe complete quenching either in the nozzle or directly at its exit, while the pressure difference between the two chambers, and thus the jet velocity, are high. When the pressure difference reduces we observe a reactive jet exiting the nozzle, which quenches downstream, again indicating quenching through mixing. Finally, despite similar phenomenology, case 3 re-ignites faster than case 2, highlighting the effect of temperature on the re-ignition propensity of the burned/unburned mixture created.

Using the 0-D model described previously, we are able to compare the different cases. To do this, the 0-D model was tuned in order to match the pressure difference over time between the two chambers. Figure 6 shows the average (dashed-dotted red line) and variation (red area) experimental pressure difference for cases 1 and 3, while the modelled pressure difference is shown in blue. Although in case1 the pressure difference is of the order of the pressure sensor noise, it can still be seen that a peak is obtained around 5.5 ms after spark timing, and that the 0-D model prediction is close to this value. In both cases very good agreement of the maximum pressure difference both in terms of peak and timing is obtained. It should be mentioned that for all the simulations performed, the model parameters were fixed to their optimum value, and no case-to-case tuning was performed.

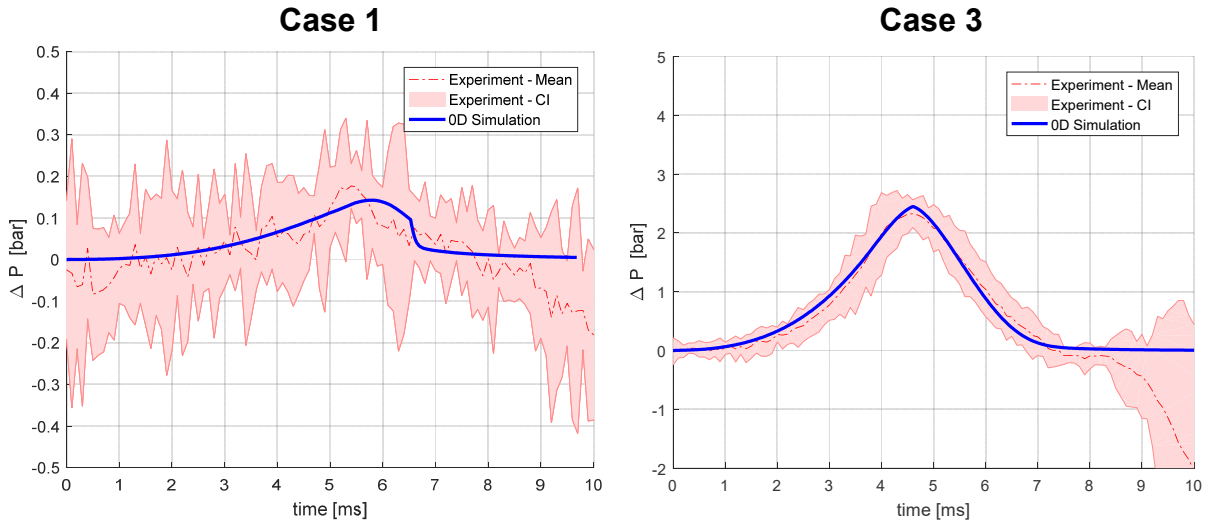

Figure 6: Exemplary comparison of experimental and simulated pressure difference between the pre- and main chambers for the OPC cases 1 and 3

Using the conditions estimated by the 0-D model, it is possible to evaluate the flame thickness for the OPC cases. The quenching distance is then:

$$\delta_q \approx 10\, l_f \approx 0.4\, mm, \text{ for case 1 and 2}$$

And

$$\delta_q \approx 10\, l_f \approx 0.35\, mm, \text{ for case 3}$$

In all cases the quenching distance is much smaller than the nozzle diameter (D_{noz}=4 mm in case 1 and 2 mm in cases 2 and 3). This means that based in this simplistic evaluation, under these thermochemical conditions thermal quenching is not expected.

The 0-D model can also be used to evaluate the evolution of the Damköhler number in time for a fixed jet position (five nozzle-diameters downstream nozzle exit). Figure 7 shows the evolution of the mixing state (blue, solid) and the flame reactivity (blue, dashed) timescales, as well as the resulting flame Damköhler number (red). In all cases the mixing timescale and thus the resulting Damköhler number starts from low values and then increases due to a reduction of the jet velocity, and thus turbulent intensity. For the larger nozzle in case 1, the initial Damköhler number is higher than in the other two cases ($Da_{fl,1}$=0.5, $Da_{fl,2}$=0.075, $Da_{fl,3}$=0.1), indicating lower quenching propensity. The lower Da_{fl} in case 2 compared to case 3 is due to the lower reactivity of the mixture, as a result of the lower temperature. Interestingly, in cases 2 and 3 the experiments show an appearance of the OH* signal when the Da_{fl} reaches a value of ~0.15. In all, the combination of the analysis using the 0-D model and the experiments indicate that at Da~0.5 the flame downstream of the nozzle is quenched, which means that a subsequent re-ignition is necessary.

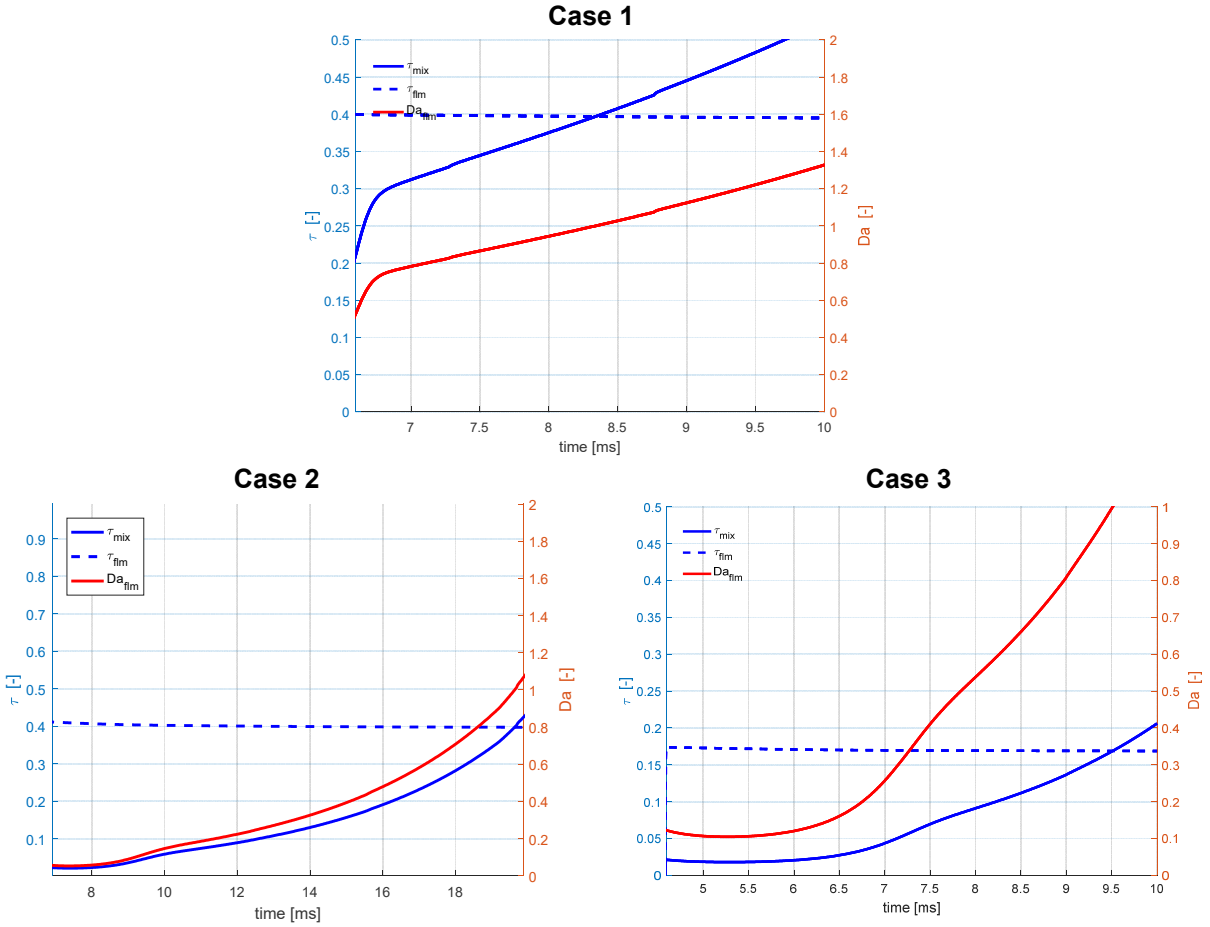

Figure 7: Evolution of mixing (blue, solid) and flame reactivity (blue, dashed) timescales, and the resulting flame Damköhler number (red) for the OPC cases 1-3

In order to study the re-ignition process, the perfectly stirred reactor calculations for various burned/unburned mixture compositions were used. The results are presented

in *Figure 8*. The plot clearly shows the combined effect of mixing (movement towards lower mixture fractions) and mixture reactivity (unburned gas temperature). In case 1, lower mixing rates are expected to result in higher mixture fractions, resulting in shorter ignition delays, as observed. In cases 2 and 3, similar mixing is observed, but the difference in the ignition delay observed (~9 vs ~4 ms after jet exit) is the result of the nearly half-order of magnitude difference in ignition delay at a constant mixture fraction. *Figure 8* also includes the ignition delay for the case of lean composition in the prechamber (Φ_{MC}=Φ_{MC}=0.75); this shows the effect of differences in the temperature of the prechamber products on ignition.

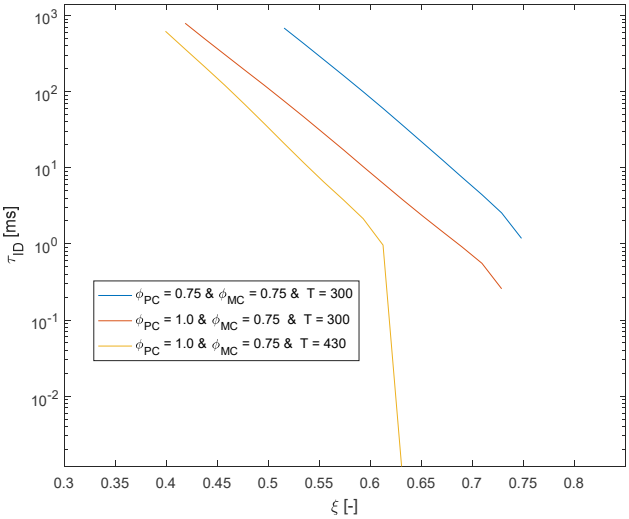

Figure 8: Ignition delay calculated using perfectly stirred reactors at different states of mixing between unburned mixture from the main chamber (ξ=0) and burned products from the prechamber (ξ=1), for different pre- and main chamber compositions and unburned temperatures

5.2 Engine application

The same analysis which was conducted for the optical prechamber can also be performed for engine applications. This will allow the estimation of the propensity for flame quenching due to thermal losses or mixing, and provide an estimate for re-ignition in cases where quenching might be present. Using the tuned 0-D engine model for the Liebherr engine, the parameters relevant for thermal and mixing-induced quenching were calculated, and are included in Table 3. The operating conditions chosen were a reference condition at high load, a condition where a prechamber with higher nozzle area (A_{noz}) to prechamber volume (V_{pc}) ratio was used, and a point at low load operation.

Table 3. Operating conditions and quenching parameter results for a typical unscavenged prechamber lean-burn engine

Operating condition	P_{sp} (bar)	T_u (K)	λ	l_f (mm)	δ_q (mm)	τ_{mix} (ms)	τ_{fl} (ms)	Da_{fl}
Reference	76	814	1.7	0.016	0.16	0.032	0.16	0.2
High A_{noz}/V_{pc}	63	813	1.7	0.016	0.16	0.075	0.15	0.5
Low load	38	810	1.7	0.023	0.23	0.036	0.16	0.225

The engine results show smaller flame thicknesses compared to the OPC, as expected from the significantly higher pressure. This results in low tendency to quench due to thermal losses in the nozzle, since the resulting quenching distance is significantly lower than the nozzle dimension. In fact, for most engine applications the pressure at ignition is expected to be significantly above the conditions tested in the OPC, which means that barring very small prechamber nozzles, thermal quenching should not be expected. At lower loads the tendency for thermal quenching will increase, but it is expected to not be important.

In terms of the calculated flame Damköhler number, in all cases simulated here the values are similar to the OPC. As expected, with higher A_{noz}/V_{pc}, the Da_{fl} reduces, due to reduced jet velocity and resulting mixing. At low loads the Da_{fl} also reduces slightly, as a result of slightly lower mixing due to lower pressure difference over the nozzle. In all, the Damköhler values observed, when compared to the values from the OPC, indicate that even for this unscanvenged prechamber application flame quenching due to mixing could be expected. Considering the higher jet velocities observed from scavenged prechambers, it seems plausible to also expect high quenching tendencies due to mixing in the jet exit in such applications. With reducing load, the quenching tendency is expected to reduce, but only slightly as was observed in this study.

Considering that flame quenching is expected, it is interesting to study the expected ignition delay. Similarly to the results shown in *Figure 8* for the OPC, Figure 9 shows the calculated ignition delays for different charge pressures, for a constant composition of equal burned and unburned gas mass fractions (ξ=0.5). The different lines present reference conditions (blue, solid – T=800K, λ=1.7), different unburned gas temperatures (magenta, dotted/dashed – T=600K, λ=1.7; green, dashed – T=700K, λ=1.7) and different charge composition (red, dotted – T=700K, λ=1.0). The variation in pressure was chosen since this will be the major alteration when varying the engine load (low load: lower pressure). The changes in unburned temperature represent engine designs with lower compression ratio, or cold starts. The case with stoichiometric operation was chosen as representative for automotive/mobile applications using a 3-way catalyst.

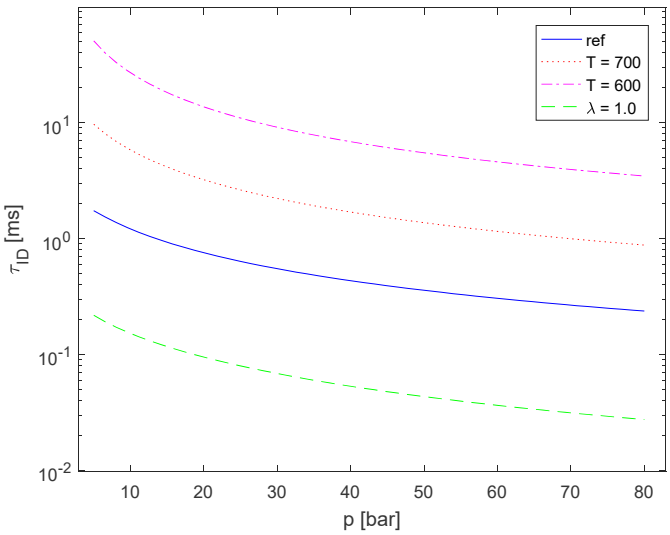

Figure 9: Ignition delay calculated using perfectly stirred reactors with equal burned/unburned mass fractions (ξ=0.5), for different mixture compositions and unburned gas temperatures. Reference T=800K, λ=1.7

The results show that the times for re-ignition are significantly shorter than observed for the OPC, as expected due to the higher temperature and pressure in the engine application. For the conditions encountered in the Liebherr engine at full load, ID for this mixture fraction is expected to be around 0.2 ms, which can be assumed to be negligible for any application, especially since the time needed to reach this level of mixing will probably be longer. Even for very low loads (10 bar, throttled operation), the ignition delay rises to around 1 ms, which is still very short compared to the OPC. This means that even if quenching takes place in such an engine application, the re-ignition will be fast enough for quenching not to be observable.

With lower charge temperatures (700 K and 600 K), the ignition delay increases significantly. This means that for engines with low compression ratios, flame quenching is expected to be more apparent. In addition, during cold start, engines with prechambers might have difficulties to ignite the main chamber mixture, depending on whether quenching is experienced and sufficient temperature and pressure is built up during compression. This provides perhaps a guideline for prechamber design, to allow engine cold-start and a wide operating range. For the stoichiometric engine application, the observed ignition delay is significantly shorter, signifying possibly reduced effect of flame quenching for such engines.

6 Conclusions

The present work uses experimental results from a generic, optically accessible prechamber test-rig, coupled to 0-D simulations of the setup as well as from a typical lean burn engine, to study the expected effect of flame quenching in prechamber applications. The generic test-rig used, called the optically accessible prechamber (OPC), allows the investigation of turbulent jet ignition under different initial pressure, temperature, composition and resulting jet velocities (through changes in the nozzle diameter). These variations enable the investigation of flame quenching and re-ignition under different thermochemical and mixing conditions. A 0-D model of the prechamber combustion and the jet formed, in combination with detailed flame and ignition chemistry calculations, allow the determination of flame quenching propensity as a result of heat losses to the nozzle wall and mixing, as well as the expected re-ignition.

The results from the OPC show that quenching is observed under all conditions presented. With a large nozzle, quenching is only observed at the tip of the hot jet, indicating quenching due to mixing of the exiting hot jet with colder reactants in the main chamber. With a smaller nozzle, resulting in very high jet velocities, no OH* signal is apparent in the hot jet, indicating quenching. In all cases flame thickness is sufficiently small and hence no flame quenching due to heat losses in the nozzle is expected. The calculated flame Damköhler number decreases with smaller nozzle diameter due to faster jet mixing, and increases with time due to the reduction of the pressure difference between pre- and main chamber, and thus the jet velocity. After some time in cases with smaller nozzle diameter, OH* appears near the nozzle, as a result of reduced mixing in that location with unburned gases. The time taken for main chamber re-ignition is strongly affected by the reactivity of the mixture, with higher temperature leading to significantly shorter ignition delay.

The application of the same methodology for quenching analysis to engine applications shows that flame quenching due to mixing can also be expected. Small flame thickness at high pressures encountered in engine do not favor flame quenching due to heat losses. For the heavy-duty/medium speed lean burn gas engine examined in this work, the flame Damköhler number was similar to the OPC, with low influence of load on the result, leading to the expectation of flame quenching due to mixing. Nevertheless, especially at conditions prevalent during high load operation and for stoichiometric engine operation (automotive/on-road applications), re-ignition in cases where quenching appears should be sufficiently fast for quenching to be not observable for most practical applications. Low-load and cold-start operation might be more demanding, due to the exponential dependency of ignition on temperature, and the resulting long ignition delays under these operating conditions. This dependency should be taken into account when prechamber engines are designed, in order to avoid ignition problems. The above analysis provides a basis to support the use of turbulent flame speed closures which do not model flame quenching, since its effect is expected to not be appreciable in most engine applications.

In all, it has been shown that the OPC is a useful test-rig for fundamental turbulent jet ignition studies. It can be used to approximate jet mixing conditions similar to those encountered in engines, and allows the study of flame quenching and re-ignition. Due to its high optical accessibility and precise setting of conditions, in addition to the lower charge ignition reactivity, this test-setup is appropriate for the study of flame quenching due to mixing, without the immediate influence of re-ignition present under high temperature and pressure conditions encountered in engines.

In terms of future work, CFD investigations, including 2D and 3D Direct Numerical Simulations, are underway in order to provide more insight into local mixing and detailed understanding of the processes observed. In addition, further experiments in the OPC are planned to expand the knowledge obtained from the investigations conducted to date.

Literature

[1] Toulson, E., Schock, H.J., Attard, W.P., *A Review of Pre-Chamber Initiated Jet Ignition Combustion Systems.* 2010. 2010-01-2263. SAE International.

[2] Dale, J.D., Checkel, M.D., Smy, P.R., *Application of high energy ignition systems to engines.* Progress in Energy and Combustion Science, 1997. 23(5–6): p. 379-398.

[3] Morsy, M.H., *Review and recent developments of laser ignition for internal combustion engines applications.* Renewable and Sustainable Energy Reviews, 2012. 16(7): p. 4849-4875.

[4] Biswas, S., et al., *On ignition mechanisms of premixed CH4/air and H2/air using a hot turbulent jet generated by pre-chamber combustion.* Applied Thermal Engineering, 2016. 106: p. 925-937.

[5] Yamaguchi, S., Ohiwa, N., Hasegawa, T., *Ignition and burning process in a divided chamber bomb.* Combustion and Flame, 1985. 59(2): p. 177-187.

[6] Carpio, J., et al., *Critical radius for hot-jet ignition of hydrogen–air mixtures.* International Journal of Hydrogen Energy, 2013. 38(7): p. 3105-3109.

[7] Iglesias, I., et al., *Numerical analyses of deflagration initiation by a hot jet.* Combustion Theory and Modelling, 2012. 16(6): p. 994-1010.

[8] Kotzagianni, M., et al., *Experimental and Computational Investigations of Prechamber Jet Ignition in a Rapid Compression Expansion Machine 10th Mediterranean Combustion Symposium*. 2017. Naples, Italy.

[9] Toulson, E., et al., *Visualization of Propane and Natural Gas Spark Ignition and Turbulent Jet Ignition Combustion.* 2012.

[10] Schlatter, S., et al., *Comparative Study of Ignition Systems for Lean Burn Gas Engines in an Optically Accessible Rapid Compression Expansion Machine.* 2013. 2013-24-0112. SAE International.

[11] Gentz, G., et al., *A study of the influence of orifice diameter on a turbulent jet ignition system through combustion visualization and performance characterization in a rapid compression machine.* Applied Thermal Engineering, 2015. 81(Supplement C): p. 399-411.

[12] Gentz, G., et al., *Combustion Visualization, Performance, and CFD Modeling of a Pre-Chamber Turbulent Jet Ignition System in a Rapid Compression Machine.* 2015.

[13] Toulson, E., Watson, H.C., Attard, W.P., *Modeling Alternative Prechamber Fuels in Jet Assisted Ignition of Gasoline and LPG.* SAE Technical Paper 2009-01-0721, 2009.

[14] Sidey, J.,Mastorakos, E., *Pre-chamber ignition mechanism: simulations of transient autoignition in a mixing layer between reactants and partially-burnt products. 10th Mediterranean Combustion Symposium*. 2017.

[15] XU, G., et al., *Experimental and Numerical Investigation of the Engine Operational Conditions' Influences on a Small Un-Scavenged Pre-Chamber's Behavior.* SAE International Journal of Engines, 2017. 10(5).

[16] Xu, G., et al., *Characterization of combustion in a gas engine ignited using a small un-scavenged pre-chamber.* International Journal of Engine Research. 0(0): p. 1468087418798918.

[17] Sadanandan, R., et al., *Detailed investigation of ignition by hot gas jets.* Proceedings of the Combustion Institute, 2007. 31(1): p. 719-726.

[18] Mastorakos, E., et al., *Fundamental Aspects of Jet Ignition for Natural Gas Engines.* SAE Int. J. of Engines 2017-24-0097, 2017. 10(5).

[19] Allison, P., et al., *Pre-Chamber Ignition Mechanism: Experiments and Simulations on Turbulent Jet Flame Structure. 10th Mediterranean Combustion Symposium*. 2017.

[20] Xu, G., et al., *Experimental and numerical investigations of the unscavenged prechamber combustion in a rapid compression and expansion machine under engine-like conditions.* Combustion and Flame, under review.

[21] Kotzagianni, M., et al., *Optical investigations of prechamber turbulent jet ignition in a rapid compression expansion machine: Influence of geometrical characteristics and conditions on cycle-to-cycle variability.* Applied Thermal Engineering, in preparation.

[22] Bardis, K., et al., *Development of a Zero Dimensional Turbulence and Heat Transfer Phenomenological Model for Pre-Chamber Gas Engines.* 2018. SAE Technical Paper 2018-01-1453.

[23] Boust, B., et al., *A thermal formulation for single-wall quenching of transient laminar flames.* Combustion and Flame, 2007. 149(3): p. 286-294.

[24] Lockwood, F.C.,Naguib, A.S., *The prediction of the fluctuations in the properties of free, round-jet, turbulent, diffusion flames.* Combustion and Flame, 1975. 24: p. 109-124.

[25] Uzun, A.,Hussaini, M.Y., *Investigation of high frequency noise generation in the near-nozzle region of a jet using large eddy simulation.* Theoretical and Computational Fluid Dynamics, 2007. 21(4): p. 291-321.

[26] Wang, N., et al., *A numerical study of the combustion and jet characteristics of a hydrogen fueled turbulent hot-jet ignition (THJI) chamber.* International Journal of Hydrogen Energy, 2018.

Acknowledgements

The authors would like to acknowledge the support of Liebherr Machines Bulle SA and the Swiss Commission for Technology and Innovation CTI (KTI-Nr. 17565.1 PFEN−IW), the Swiss Federal Office of Energy (grant no. SI/501584-01 and IEA GECT operating agent), the Swiss Competence Centre for Energy Research – Efficient Technologies and Systems for Mobility (SCCER-Mobility) and European Union's Horizon 2020 GASON research and innovation programme under grant agreement No 652816.